UC Davis
UC Davis Previously Published Works

Title

The anatomical and compositional basis of leaf mass per area

Permalink

Journal

ISSN

Authors

John, Grace P
Scoffoni, Christine
Buckley, Thomas N
et al.

Publication Date

DOI

Peer reviewed

LETTER

The anatomical and compositional basis of leaf mass per area

Grace P. John,[1] Christine Scoffoni,[1] Thomas N. Buckley,[2] Rafael Villar,[3] Hendrik Poorter[4] and Lawren Sack[1]*

Abstract

Leaf dry mass per unit leaf area (LMA) is a central trait in ecology, but its anatomical and compositional basis has been unclear. An explicit mathematical and physical framework for quantifying the cell and tissue determinants of LMA will enable tests of their influence on species, communities and ecosystems. We present an approach to explaining LMA from the numbers, dimensions and mass densities of leaf cells and tissues, which provided unprecedented explanatory power for 11 broadleaved woody angiosperm species diverse in LMA (33–262 g m^{-2}; $R^2 = 0.94$; $P < 0.001$). Across these diverse species, and in a larger comparison of evergreen vs. deciduous angiosperms, high LMA resulted principally from larger cell sizes, greater major vein allocation, greater numbers of mesophyll cell layers and higher cell mass densities. This explicit approach enables relating leaf anatomy and composition to a wide range of processes in physiological, evolutionary, community and macroecology.

Keywords

Deciduous, evergreen, functional traits, leaf anatomy, leaf density, leaf economics, leaf thickness, mesophyll, SLA, specific leaf area.

Ecology Letters (2017) **20**: 412–425

INTRODUCTION

A grand challenge in plant ecology is to simplify the diversity of plant structure and ecological specialisation by identifying underlying patterns. One of the best recognised is the 'leaf economic spectrum' (LES). Central to the LES is leaf lamina dry mass per unit leaf area (LMA), which is negatively related across diverse species to photosynthetic and respiration rates and leaf nitrogen concentration per unit leaf mass and positively related to leaf lifespan (Small 1972; Reich *et al.* 1997; Wright *et al.* 2004). Although LES relationships may be weak in given species sets (Funk & Cornwell 2013; Mason & Donovan 2015; Grubb 2016), across diverse species a high LMA is typical for slow growing or stress tolerant species and low LMA for rapidly growing species (Poorter & Van der Werf 1998; Wright *et al.* 2004; Adler *et al.* 2014; Reich 2014; Diaz *et al.* 2016; Kunstler *et al.* 2016). LMA holds an importance in plant ecology similar to that of body size in animal ecology (Reich 2001;Westoby *et al.* 2002). A quantitative framework resolving the structural and compositional basis for LMA would contribute strongly to the ability to resolve the role of cell and tissue-level traits in driving ecological processes across scales (e.g. Niinemets 2001; Blonder *et al.* 2011; Herben *et al.* 2012; Villar *et al.* 2013; Wang *et al.* 2015) as well as understanding how genetic and developmental processes constrain trait variation across species (Sack *et al.* 2012; Mason & Donovan 2015).

Many studies have related LMA to gross leaf structure, i.e. to leaf area (LA) and mass (LM), given that LMA = LM/LA, or to leaf thickness (LT) and dry mass density (LD, i.e. dry mass per hydrated volume), given that LMA = LT × LD (Witkowski & Lamont 1991; Shipley 1995; Niinemets 1999; Poorter *et al.* 2009). Gross leaf structure can influence other leaf biomechanics and ecological processes such as decomposition rates (Cornelissen & Thompson 1997; Cornwell *et al.* 2008; Onoda *et al.* 2011). However, it is not possible to infer how anatomy and composition determine LMA from these gross structural variables because given anatomical traits can have contradictory impacts on LA and LM, or on LT and LD (Niinemets 1999). A more detailed approach is necessary to understand the influence of cell and tissue traits on LMA and thereby potentially on higher level ecological processes. Previous studies provided important insights into species variation in LMA by partitioning the volume and mass by air, water and solid fractions (Roderick *et al.* 1999a,b; Sack *et al.* 2003), or by analysing correlations of LMA with given anatomical variables (Table 1). Published hypotheses and models posit that high LMA for a given species is driven by smaller cells (Shipley *et al.* 2006; Villar *et al.* 2013) or larger cells (Pyankov *et al.* 1999); by low airspace fraction (Roderick *et al.* 1999b; Sack *et al.* 2003); or by high or low vein length per unit area (vein density) (Blonder *et al.* 2011). These hypotheses have not been consistently supported in tests across diverse sets of species (Table 1), highlighting a critical need for an explicit framework for resolving the underlying basis for LMA.

[1]*Department of Ecology and Evolutionary Biology, University of California Los Angeles, 621 Charles E. Young Drive South, Los Angeles, CA 90095, USA*
[2]*Plant Breeding Institute, Sydney Institute of Agriculture, The University of Sydney, 12656, Newell Hwy, Narrabri, NSW 2390, Australia*
[3]*Área de Ecología, Universidad de Córdoba, Edificio Celestino Mutis, Campus de Rabanales, 14071 Córdoba, Spain*

[4]*Plant Sciences (IBG2), Forschungszentrum Jülich GmbH, D-52425 Jülich, Germany*
Correspondence: lawrensack@ucla.edu
All data included as supplement and will be deposited into larger databases.

Table 1 Studies of correlations of leaf mass per area (LMA) with anatomy across species, emphasising the contrasting results, and the mismatch of correlation with the causal influences shown by sensitivity analyses using the EXACT equations (Box 1; Fig. 2c–e)

Authors	Species tested and range of species mean LMA values (g m^{-2})	Tissue thicknesses	Cell size	Number of cells per area	Number of cell layers	Airspace fraction	Vein traits
This study	11 woody species (33.2–262)	UC (+0.78), UE(ns), PA(+0.81), SP(+0.82), LE(ns), LC (ns)	CV$_{ue}$ (ns), CV$_{pa}$ (ns), CV$_{sp}$ (ns), CV$_{le}$ (ns), CV$_{bs}$ (ns), CV$_{bse}$ (ns)	UE (ns), PA (ns), SP (ns), LE (ns), BS (ns), BSE (ns), Total (ns)	UE (+0.61), PA(+0.65), SP(+0.77), LE(ns)	AF$_{pa}$ (ns), AF$_{sp}$ (ns), AF (ns)	VD$_{1°}$ (ns), VD$_{2°}$ (ns), VD$_{3°}$ (ns), VPA$_{1°}$ (+0.66), VPA$_{2°}$ (+0.78), VPA$_{3°}$ (ns), VPA$_{min}$ (ns), VPA$_{maj}$ (+0.77), VLA$_{min}$ (ns)
Aranda et al. (2004)*	8 temperate species, data corrected for canopy irradiance (62.7–175)	UE (+0.80), PA (+0.84), SP (+0.95), LE (ns)					
Blonder et al. (2011)*	25 woody species (25.2–245)						VLA$_{min}$ (−0.41), IVD (ns)
Blonder et al. (2016)	32 Hawaiian silversword alliance taxa (19.7–620)						VLA$_{min}$ (0.41)
Brodribb et al. (2013)	48 Proteaceae species (94–288)		CD$_{pa}$ and CD$_{ue}$ (ns)				VD$_{maj}$ (−0.29)
Castro-Diez et al. (2000)	52 European woody species (17.5–106)	VSC (i.e. veins, BS and BSEs) (+0.72), UE+LE (ns), PA (+0.37), SP (ns)	CA$_{pa}$ (ns)				
Dunbar-Co et al. (2009)	7 Hawaiian Plantago taxa (15.2–91.5)						VLA$_{maj}$, VLA$_{min}$ (ns)
de la Riva et al. (2016)	34 woody species (27.8–207)	MES (+0.84), EP (ns)				AF$_{sp}$ (+0.92)	VPA$_{vsc}$ (+0.69)
Garnier & Laurent (1994)	14 grass species (23.1–49.5)	MES (ns), EP (ns)					VPA$_{tv}$ (+0.61), VPA$_{vsc}$ (+0.66), VPA$_{tv}$ + VPA$_{vsc}$ (+0.71)
Kawai and Okada (2016)	8 Fagaceae species (70.9–174)						VLA$_{1° + 2°}$ (+0.83), VLA$_{min}$ (ns)
Li et al. (2015)	85 sub-tropical and tropical Chinese species (33–159)						VLA$_{tv}$ (ns)
Mediavilla et al. (2001)*	6 woody deciduous species (121–242)	TC (+0.94), PA (ns), SP (ns), EP (ns), PA (0.88) SP (ns)					
Nardini et al. (2012)*	3 species of Quercus and 3 species of Acer (44.2–115)						VLA$_{tv}$ (ns),

Table 1. (continued)

Authors	Species tested and range of species mean LMA values (g m^{-2})	Tissue thicknesses	Cell size	Number of cells per area	Number of cell layers	Airspace fraction	Vein traits
Pyankov et al. (1999)*	94 vascular plant species (293–1826)		CV$_{mes}$ (+0.26)	Total (ns)			
Ronzhina & Ivanov (2014)	19 species of aquatic higher plants (8.4–72.8)			Total (+0.65)			
Sack et al. (2013; 2014)	275 dicotyledonous species (25–605)						VLA$_{maj}$ (across 58 species, + 0.38) VLA$_{tv}$ (all species, ns)
Scoffoni et al. (2015)	6 species of Hawaiian lobeliads, high irradiance treatment (77.9–605)	UC (+0.87), LC (ns), UE (−0.83), LE (ns), SP (ns), PA (ns)	CA$_{ue}$, CA$_{le}$, CA$_{pa}$, CA$_{sp}$, CA$_{bs}$, (ns)		SP (ns), PA (ns)	AF$_{sp}$ (ns), AF$_{pa}$ (ns), AF (ns)	VLA$_{maj}$ (+0.93), VLA$_{min}$ (ns), VLA$_{tv}$ (ns)
Tomás et al. (2013)	15 species of dicotyledonous herbs and trees (20.7–123)	SP (+0.54), PA (+0.24)			PA (+0.63)		
Van Arendonk et al. (1997)	4 species of Poa grown under three nitrogen supplies (18.1–27.3)		CA$_{ep}$ (+0.72), CA$_{vsc}$ (ns)				
Van Arendonk & Poorter (1994)	14 grass species (20.9–39.5)		CA$_{ep}$ (+0.64), CA$_{vsc}$ (ns)			AF†$^{(ns)}$	
Villar et al. (2013)*	26 woody species (31.5–151)	EP (ns), MES(+0.77)	CA$_{ep}$ (−0.53), CA$_{mes}$ (ns)			AF$_{sp}$(ns)	VPA$_{vsc}$(+0.62)
Xiong et al. (2015)	11 taxa of Oryza (24.6–45.3)						VLA$_{tv}$ (ns)

Correlation coefficients are reported for tissue thickness, cell sizes, cell numbers per area, airspace fractions, and vein traits. Symbols for tissues: UC, upper (adaxial) cuticle, UE, upper epidermis; PA, palisade mesophyll; SP, spongy mesophyll; LE, lower (abaxial) epidermis; LC, lower cuticle; BS, bundle sheath; BSE, bundle sheath extensions; VSC, vascular schlerenchyma; MES, entire mesophyll; EP, total epidermis; and TC, total cuticle. Cell sizes were reported as diameter (CD), cross-sectional area (CA), or volume (CV). Air fractions were reported as fraction of thickness or volume of the whole mesophyll (AF), the spongy mesophyll (AF$_{sp}$), or the palisade mesophyll (AF$_{pa}$). Studies reporting airspace data were included only when airspace was measured anatomically, i.e. not when estimated gravimetrically. Vein traits included vein length per area (VLA), vein diameter (VD), vein volume per area (VPA) and interveinal distance (IVD) and subscripts give specific vein branching orders tested or maj for major veins (first-, second- and third-order), min for minor veins (fourth and higher order), vsc for vascular schlerenchyma, or tv for total vein system. + positive correlation; − negative correlation.
*Some or all the correlations presented are results of our analyses of the published data.
†Airspace calculated as a fraction of entire cross section (i.e. including epidermis, cuticle and vascular tissues).

Table 2 Leaf traits contributing to leaf mass per area (LMA) in the EXACT approach, and additional traits considered when scaling up from LMA to other physiological traits

Trait	Symbol	Practical units	Formula units	Tissues
Leaf tissue and cell traits in the EXACT approach				
Cell volume	CV_x	μm^3	m^3	ue, pa, sp, bs, bse, le
Number of cells per leaf area	NCA_x	# μm^{-2}	# m^{-2}	ue, pa, bs, bse, sp, le
Volume of tissue per leaf area (non-airspace)	VPA_x	$\mu m^3\ \mu m^{-2}$	$m^3\ m^{-2}$	uc, ue, pa, bs, bse, sp, le, lc, 1°, 2°, 3°, min
Tissue dry mass density	ρ_x	g cm^{-3}	kg m^{-3}	uc, lc, tc, v
Cell dry mass density	ρ_{cell}	g cm^{-3}	kg m^{-3}	ue, pa, bs, bse, sp, le, cell
Tissue mass per leaf area	TMA_x	g m^{-2}	g m^{-2}	uc, ue, pa, bs, bse, sp, le, lc, v, tc
Additional traits used to calculate NCA				
Cell height	CH_x	μm	m	ue pa, le
Cell diameter	CD_x	μm	m	ue, pa, sp, le
Number of cell layers	NCL_x	# μm^{-2}	# m^{-2}	ue, pa, sp, le
Air space fraction	AF_x	%	%	pa, sp
Tissue cross-sectional area	A_x	μm^2	m^2	bs, bse
Vein diameter	VD_x	μm	m	1°, 2°, 3°, min
Vein length per area	VLA_x	mm mm^{-2}	mm mm^{-2}	1°, 2°, 3°, min
Percent of vein volume protruding from lamina	$\%VPA_{prox}$	%	%	1°, 2°, 3°
Volume of vein embedded in leaf per leaf area	VPA_{emx}	$mm^3\ mm^{-2}$	$m^3\ m^{-2}$	1°, 2°, 3°
Leaf economic and growth traits				
Leaf area	LA	cm^2	m^2	
Leaf thickness	LT	μm	m	
Leaf dry mass density	LD	g m^{-2}	kg m^{-3}	
Leaf mass per area	LMA	g m^{-2}	kg m^{-2}	
Leaf lifespan	LL	months		
Photosynthetic assimilation rate per leaf mass	A_{mass}	nmol $g^{-1}\ s^{-1}$		
Nitrogen concentration per leaf mass	N_{mass}	%		
Respiration rate per leaf mass	R_{mass}	nmol $g^{-1}\ s^{-1}$		

We provide trait symbols, the units in which each trait is typically considered, the units used in the equations and the tissues for which these traits are inputted. Traits featuring a subscript (x) represent tissue specific values. Tissues include upper cuticle (uc), upper epidermis (ue), palisade mesophyll (pa), spongy mesophyll (sp), bundle sheath (bs), bundle sheath extension (bse), lower epidermis (le), lower cuticle (lc), first-, second- and third-order veins (1°, 2°, 3°), minor veins (min), total cuticle (tc) and total veins (v) and volume-weighted average across all non-vascular cells (cell). Note that Table 2 only includes parameters used in the EXACT approach; parameters used in the consideration of alternative models for LMA are not included (see Methods S4 and Table S5).

We developed an approach to explain LMA from underlying anatomical and compositional determinants – the volumes and mass densities of cells and tissues. We named this approach in aspirational terms the 'Exhaustive Anatomy and Composition of Tissues (EXACT)' approach (Fig. 1a–d; Box 1), as it can be applied with simplifications or elaborated to the finest possible detail. While some previous studies have estimated the contributions of given tissues to LMA by fitting statistical relationships (Poorter *et al.* 2009; Villar *et al.* 2013) or drawn inferences from models that included few traits (Shipley *et al.* 2006; Blonder *et al.* 2011), our approach is a radical departure based on fully explicit mathematical and physical relationships. We applied a simplified version of the EXACT approach in six ways: (1) to test the degree that LMA can be explained from cell and tissue anatomy and composition, (2) to compare its performance with that of antecedent models that explained LMA from few traits, (3) to partition the leaf mass and volume into tissues, (4) to establish the anatomical and compositional basis for differences in LMA across species, and (5) across evergreen and deciduous leaf types and (6) to examine the potential for cell anatomy and composition to scale up via LMA to an influence on global leaf economic trait relationships.

MATERIALS AND METHODS

Species selection

To test the EXACT approach (Box 1; Fig. 1a–d) and other models, we made detailed measurements of leaf anatomy and composition for 11 simple-leaved woody angiosperm species selected for morphological, phylogenetic and ecological diversity: *Bauhinia galpinii, Camellia sasanqua, Cercocarpus betuloides, Hedera canariensis, Heteromeles arbutifolia, Lantana camara, Magnolia grandiflora, Platanus racemosa, Quercus agrifolia* and *Raphiolepis indica* (Table S2). We followed earlier studies focusing on laborious measurements for relatively few species spanning a wide range of values for the study variable (Table 1; Methods S1); this approach can later be applied to larger species sets from broader phylogenetic or life history groups (e.g. gymnosperms, herbs) across different biomes. We sampled plants cultivated in or surrounding the University of California, Los Angeles and at Will Rogers State Park (*Quercus agrifolia*). Mature, sun-exposed leaves were collected from three mature individuals of each species between September 2011 and April 2014. Branches were transported to the laboratory in plastic bags with wet paper towels, recut under water by at least two nodes, and rehydrated overnight with stems underwater and
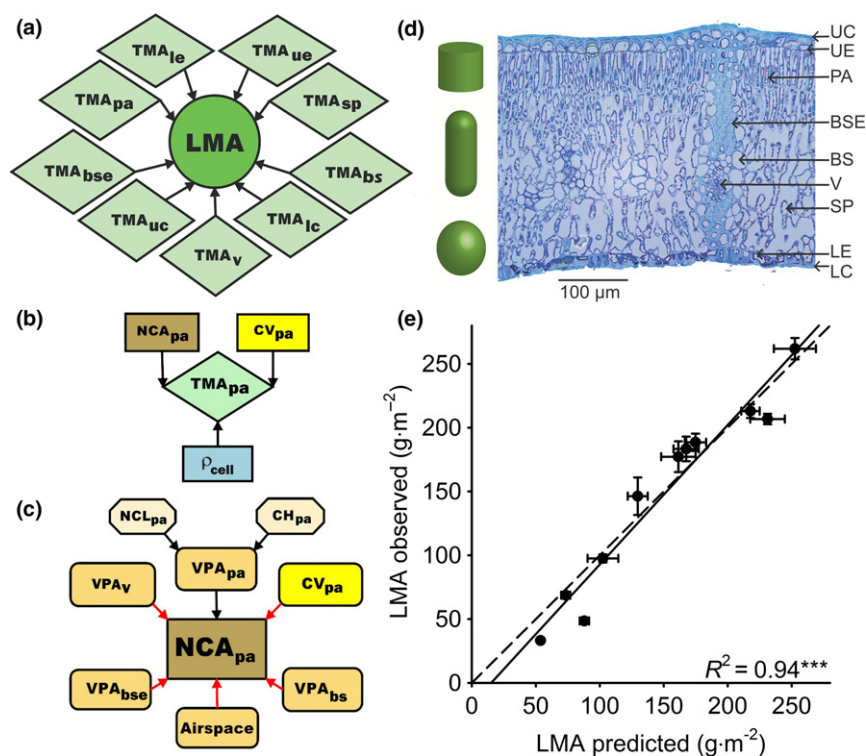
Figure 1 Analysing the basis for leaf mass per area (LMA) according to an Exhaustive Anatomy and Composition of Tissues (EXACT) approach. (a) LMA is the sum of the values of tissue mass per area (TMA) for all the component leaf tissues, including upper cuticle (UC), palisade mesophyll (PA), bundle sheath extensions (BSE), bundle sheath (BS), vascular tissue (V), spongy mesophyll (SP), lower epidermis (LE) and lower cuticle (LC). (b) For epidermal and mesophyll tissues, TMA is a positive function of cell volume (CV), the number of cells per leaf area (NCA) and the relevant tissue dry mass density (ρ_{cell}). (c) In turn, NCA is a positive function of the tissue volume per area (VPA, i.e. tissue thickness, itself a positive function of number of cell layers (NCL) and cell height (CH)), and the NCA of mesophyll tissues (pa) is also a negative function (red arrows) of the vein volume (VPA_v), airspace fraction (AF) and the volumes of bundle sheath (VPA_{bs}) and bundle sheath extensions (VPA_{bse}) as these all must be subtracted from the tissue thickness to estimate the cellular volume (CV), (d) Tissue and cell volumes were determined from transverse cross sections, as in this example for *Quercus agrifolia*; epidermal, palisade mesophyll and spongy mesophyll cells were modelled respectively as cylinders, capsules and spheres. (e) The prediction of LMA using EXACT Eqn 7 based on anatomical traits for 11 diverse woody broadleaf angiosperm species, using only a constant value for ρ_{cell} for all lamina tissues in all species. The solid line shows regression of empirically determined values for LMA against those calculated using the EXACT approach for individual leaves then averaged by species (slope = 1.09 ± 0.09); dashed line is the 1 : 1 line. ***$P < 0.001$.

Box 1 Theory and derivation of the Exhaustive Anatomy and Composition of Tissues (EXACT) approach

(see Table 2 for summary of symbols and units)

LMA for a given leaf can be considered as the sum of its tissues (Poorter *et al.* 2009), formalised as the sum of the tissue mass of each component tissue$_x$ per projected leaf area ($TMA_{x;}$):

$$LMA = TMA_{uc} + TMA_{ue} + TMA_{pa} + TMA_{bs} + TMA_{bse} + TMA_{sp} + TMA_{le} + TMA_{lc} + TMA_v, \quad (1)$$

where subscripts uc, ue, pa, bs, bse, sp, le, lc and v represent, respectively, the upper cuticle, upper epidermis, palisade mesophyll, minor vein bundle sheath, minor vein bundle sheath extensions, spongy mesophyll, lower epidermis, lower cuticle and leaf vein tissue (Fig. 1a and d). Just as for the whole leaf, LMA = LT × LD (Witkowski & Lamont 1991), for the non-airspace component of each tissue x,

$$TMA_x = \rho \times VPA_x, \quad (2)$$

where ρ is the dry mass density (i.e. dry mass/hydrated volume) of the non-airspace component, and VPA_x the non-airspace volume of the tissue per leaf area. For epidermal and mesophyll tissues, the cellular basis can be further elaborated:

$$VPA_x = CV_x \times NCA_x \quad (3)$$

where CV_x is the mean cell volume and NCA_x the number of cells per projected one-sided surface area of leaf of a given tissue (Fig. 1b).Thus, combining eqns 1–3,

Box 1 (continued)

$$\text{LMA} = \text{VPA}_{uc}(\rho_{uc}) + \text{CV}_{ue}(\rho_{ue})\text{NCA}_{ue} + \text{CV}_{pa}(\rho_{pa})\text{NCA}_{pa} + \text{CV}_{bs}(\rho_{bs})\text{NCA}_{bs} + \text{CV}_{bse}(\rho_{bse})\text{NCA}_{bse} + \text{CV}_{sp}(\rho_{sp})\text{NCA}_{sp}$$
$$+ \text{CV}_{le}(\rho_{le})\text{NCA}_{le} + \text{VPA}_{lc}(\rho_{lc}) + \text{VPA}_{v}(\rho_{v}) \tag{4}$$

For the palisade and spongy mesophyll tissues, the NCA can be determined as the total VPA (or tissue thickness), minus the volume per area of airspace, vein, bundle sheath and bundle sheath extension tissue, and divided by CV_x (Table S1; Fig. 1c) CV_x can be estimated from cross-sectional anatomy. For simplicity, we modelled epidermal cells as cylinders, palisade mesophyll cells as capsules and spongy mesophyll cells as spheres (Nobel 2009; Chatelet *et al.* 2013) (Fig. 1d; Table S1 in Supporting Information).Note that the EXACT approach avoids inputting LT and LD directly into the estimation of LMA as the focus of this approach is for scaling from cell and tissue-level traits to LMA. Thus when estimating input traits such as VPA, the EXACT approach uses cell dimensions and numbers of layers (Eqns 2b–2g in Table S1), and not tissue thickness values. For the epidermises, and spongy and palisade mesophyll, the total VPA (or thickness) of each tissue_x is considered as:

$$\text{VPA}_x = \text{CH}_x \times \text{NCL}_x, \tag{5}$$

where CH_x is the mean cell height and NCL_x the number of cell layers, i.e. the number of horizontal rows in the tissue that may be occupied at any point by a cell (or else by airspace) in a transverse cross section of tissue_x. Consideration of cell heights and cell layers rather than thickness separates the influence of cells from airspace, enables explicit analyses of the causal influence of cell sizes on LMA, and relates LMA to causal variables with a more transparent relationship to developmental processes, i.e. the differentiation and expansion of cells and tissues. Accurate estimation of the volume per leaf area of veins (VPA_v) requires accounting explicitly for the vein system architecture with its tapering system of vein orders, from the first-order vein or veins (1°) to second- (2°) and third-order (3°) veins to minor veins. Thus, VPA_v is the sum across the number j of vein orders of the product of vein length per area (VLA) and vein cross-sectional area (VA) of the given vein orders:

$$\text{VPA}_v = \sum_{i^o=1^o}^{j^o} \text{VLA}_{i^o} \times \text{VA}_{i^o} \tag{6}$$

The EXACT approach can be simplified in many ways, allowing estimation of LMA at the level of complexity permitted by available measurements, with the ability to add greater precision with finer scale measurements. One major issue is that the mass densities of individual cell types are not directly measurable with currently available techniques. A simplified version of the approach enables estimation of LMA based on a single volume-weighted average 'bulk' cell dry mass density across epidermis and mesophyll tissues (ρ_{cell}), and a volume-weighted average dry mass density of the upper and lower cuticle (ρ_{tc}):

$$\text{LMA} = \left(\text{CV}_{ue}(\text{NCA}_{ue}) + \text{CV}_{pa}(\text{NCA}_{pa}) + \text{CV}_{bs}(\text{NCA}_{bs}) + \text{CV}_{bse}(\text{NCA}_{bse}) + \text{CV}_{sp}(\text{NCA}_{sp}) + \text{CV}_{le}(\text{NCA}_{le})\right)\rho_{cell} + (\text{VPA}_{uc}$$
$$+ \text{VPA}_{lc})\rho_{tc} + \text{VPA}_v(\rho_v) \tag{7}$$

While ρ_{cell} is not directly measurable, given that the assumptions of the EXACT approach are supported, Eqn 7 can be rearranged to allow ρ_{cell} to be inferred from measurements of LMA and anatomical variables:

$$\rho_{cell} = \frac{\text{LMA} - ((\text{VPA}_{uc} + \text{VPA}_{lc})\rho_{tc} + \text{VPA}_v(\rho_v))}{\left(\text{CV}_{ue}(\text{NCA}_{ue}) + \text{CV}_{pa}(\text{NCA}_{pa}) + \text{CV}_{bs}(\text{NCA}_{bs}) + \text{CV}_{bse}(\text{NCA}_{bse}) + \text{CV}_{sp}(\text{NCA}_{sp}) + \text{CV}_{le}(\text{NCA}_{le})\right)} \tag{8}$$

This equation enables estimation of ρ_{cell} based on measured LMA and anatomy. One may also determine the mathematical sensitivity of LMA to this parameter relative to other measured parameters and indeed, LMA does depend strongly on ρ_{cell}. However, for testing the EXACT model, we used only a constant across species for ρ_{cell}, avoiding circularity.

covered with plastic bags, so that measurements were made for turgid tissues.

Measurement of leaf mass per area and thickness

Leaves were sampled for LMA and anatomical sectioning from the same three individual plants per species, but of necessity different leaves were used. A larger leaf set was used for empirical determination of LMA and a smaller set for anatomical measurements. LMA varies considerably across sun leaves of given species; to estimate LMA for the leaves measured for anatomy, we developed empirical equations relating LMA to thickness for sun leaves of given species (Richardson *et al.* 2013). For 14–26 sun

leaves of each species we averaged turgid leaf thickness (LT) measured at the base, middle and tip between second-order veins using digital callipers ($\pm$ 0.01 mm; Fisher Scientific, PA, USA). We removed petioles with a scalpel and measured leaf area by scanning leaves (Canon Scan Lide 90; Canon USA Inc., NY, USA) and analysing the images (ImageJ software version 1.42q; National Institutes of Health). Leaf blades were dried for over 48 h at 70 °C and weighed with an analytical balance ($\pm$ 0.01 mg; MS205DU; Mettler Toledo, OH, USA). LMA was determined by dividing the leaf lamina dry mass (i.e. without petiole) by projected surface area (Perez-Harguindeguy *et al.* 2013). We fitted species-specific linearised power laws for LMA vs. LT:

$$\log(\text{LMA}) = \log(a) + b\log(\text{LT}) \tag{9}$$

where *a* and *b* were fitted parameters for each species (Table S2). For 9 of 11 species the ordinary least squares regressions were significant ($R^2 = 0.28$–0.79, $P < 0.001$–0.02; $n = 14$–26) as determined using SMATR (Warton *et al.* 2006), and allowed estimation of LMA for the leaves measured for anatomy based on their thickness. For *C. diversifolia* and *R. indica* the LMA vs. LT relationship was not significant ($R^2 = 0.07$–0.12, $P = 0.11$–0.22; $n = 23$), and mean LMA values across the sample were used.

Measurements of leaf cross-sectional anatomy

One leaf from each of three individuals per species was fixed in formalin acetic acid-alcohol solution (37% formaldehyde, glacial acetic acid, 95% ethanol and deionised water in a 10:5:50:35 mixture). Transverse cross sections of 1 µm thickness were prepared and imaged (John *et al.* 2013) to estimate the volumes of cells and tissues (Nobel 2009; Chatelet *et al.* 2013). We made measurements of cell and tissue dimensions using ImageJ software (version 1.42q; National Institutes of Health) and determined the traits listed in Table 2 (Methods S2).

Full elaboration of the calculations and assumptions used for estimating inputs for the equations, and validation of the equations, are presented in Methods S3 and Table S4.

Measurement of vein traits

We estimated volume per area for first-, second- and third-order veins and for minor veins based on vein diameters and lengths per area (VLA). We used previously published vein traits for sun leaves collected from the same individuals for nine of the 11 species (Scoffoni *et al.* 2011), assuming that temporal variation in vein traits on an individual plant would be similar to the variation among sun leaves on the same plant at a given sampling time (Uhl & Mosbrugger 1999). For the remaining two species (*Bauhinia galpinii* and *Raphiolepis indica*), we measured vein traits using the same sampling, clearing, staining and measurement protocol for three leaves per species. For one leaf sampled from each of three individuals of each of the 11 species, we estimated midrib dry mass density as a proxy for vein dry mass density (Methods S3). We estimated midrib volume by modelling the midrib as a cone with basal diameter measured at the petiole insertion, given that the midrib for many leaves is too small to measure precisely using the displacement method. We obtained midrib dry mass by excising using a scalpel and drying for 72 h at 70 °C before weighing (± 0.01 mg; MS205DU; Mettler Toledo, OH, USA), and determined dry mass density as dry mass/hydrated volume.

Comparison of EXACT approach performance with previous models predicting LMA from anatomy

We compared the EXACT approach with antecedent models that enabled a prediction of LMA on the basis of fewer traits

assumed to be primary determinants of LMA, i.e. the ratio of cell wall to cell protoplast volume (Shipley *et al.* 2006), or leaf veins (Blonder *et al.* 2011). All approaches estimate LMA directly based on inputs of anatomical measurements and constants, without fitted statistical parameters (Methods S4; Table S5). The EXACT approach would be expected to predict LMA more accurately as it includes a fully explicit formulation based on cells and tissues.

Tests of anatomical and compositional traits as determinants and correlates of LMA

We tested the influence of anatomical and compositional traits on LMA using three approaches (Methods S5; Tables S6, S7 and S8). The EXACT model for LMA is a mathematical identity, and we applied it to two types of causal analyses. First, we tested the 'intrinsic sensitivity' of LMA to each input variable in the EXACT equations by noting how LMA varied when each variable was changed by 10% of its mean value while holding all other variables at their mean values. Second, given that shifts in multiple traits in concert determine LMA variation across species, we considered how much the observed shifts in given traits actually contribute to realised species differences in LMA by partitioning the contribution of each variable to the difference in LMA (δLMA) between all possible pairwise species combinations (eqns S.8; Buckley & Diaz-Espejo 2015) and calculating the median contribution across these species combinations (Table S7). The inferred contributions thus depend entirely on the species-set considered, and we refer to these as 'realised sensitivity'. Third, we compared the intrinsic and realised sensitivity of LMA to individual traits with the observed correlations between LMA and each trait, to test for discrepancies. For example a correlation of LMA with a given trait could arise without reflecting any direct influence of the trait on LMA if that trait were correlated with another strong determinant.

To assess the representativeness of our species in their relationship of LMA to anatomy, we examined the correlations of LMA with individual traits across the published literature for woody and herbaceous plants. We conducted searches using Web of Science (using as keywords 'leaf mass per area', 'LMA', 'anatomy', 'specific leaf area', 'cell size', 'airspace', 'air space', etc.) to compile published data sets featuring measurements of LMA and anatomical traits (Table 1).

Differences among evergreen and deciduous species

LMA is generally greater in evergreen than deciduous species (Villar & Merino 2001; Gurevitch *et al.* 2002; Wright *et al.* 2004). We used the realised sensitivity analysis described above based on the EXACT equations to clarify the anatomical and compositional basis for this difference (Methods S6). We assembled available comparative anatomical data for evergreen and deciduous species beyond our 11 diverse angiosperms (i.e. total volumes per leaf area of epidermis, mesophyll, vascular sclerenchyma and airspace, and cell sizes), resulting in data for 16 deciduous and 21 evergreen species (Villar *et al.* 2006, 2013; Table S9).

Scaling up the influence of anatomical and compositional to the worldwide leaf economics spectrum

Using the EXACT equations to determine LMA from anatomical traits, we estimated their potential influence on other leaf economics spectrum (LES) traits and LES relationships using available empirical models for these processes (Supporting Information Discussion).

RESULTS

Quantitative explanation of LMA from cell and tissue-scale measurements

For 11 diverse woody species, we determined LMA and conducted detailed measurements of cross-sectional anatomy, venation architecture and tissue composition. The range of these species' LMA values, 33–262 g m^{-2}, spanned the 0.9–88th percentile for tree and shrub species in a large global database, Glopnet (LMA = 23–1501 g m^{-2}; n = 1700; Wright *et al.* 2004). We tested the explanatory power of the EXACT approach by applying Eqn 7 (i.e. the expanded form of eqn 1), to each of the three sampled leaves for each species. For this application, we set the bulk cell dry mass density in the mesophyll and epidermis (ρ_{cell}), which could not be measured directly, as the mean value for species from this study and from Villar *et al.* (2013), as determined using Eqn 8 (ρ_{cell} = 0.411 g cm^{-3}). Eqn 7 explained LMA with high accuracy and precision (R^2=0.94; P < 0.001; n = 11; Fig. 1e).

Comparison of explanatory power of the EXACT approach with that of previous models

We compared the power of the EXACT approach, using a mean ρ_{cell} across all species, with that of the three previously published models that explained LMA on the basis of fewer anatomical inputs, applied to the 11 species (Results S2; Fig. S2; Table S10). All tested models made direct predictions from anatomical measurements and assumed constants, without any fitted statistical parameters. As expected, the EXACT approach outperformed previous models, i.e. ΔAICc = 30–52, with substantially higher R^2 and without predictive bias (i.e. the slope of the line fitted with zero intercept included 1.0 in the 95% confidence intervals; Wagenmakers 2003; Table S9). In contrast with the previous models, the EXACT approach had stronger ability to predict LMA than leaf thickness (LT) alone (R^2 = 0.94 vs. R^2 = 0.63; Table S9). Even assuming a constant ρ_{cell}, the EXACT approach predicted not only LMA (Eqn 7; Fig. 1e), but LT (eqn 5 in Table S3; Fig. S3a; R^2 = 0.98; P < 0.001) and LD (Eqn 6 in Table S3; Fig. S3b; R^2 = 0.58; P = 0.04).

Partitioning the leaf volume and mass by tissues

The EXACT approach allowed decomposition of the leaf volume and mass by tissues and supported the predominant role in determining leaf volume of mesophyll cells and airspace (comprising *c.* 50%), followed by major veins and epidermis (*c.* 30%), and a far lesser role of bundle sheath, bundle sheath extensions, cuticle and minor veins (Fig. 2a; Table S11).

Under our simplifying assumptions (e.g. a constant ρ_{cell} for all species), the leaf mass was predominantly determined by the mesophyll cells and major veins (*c.* 60%), followed by epidermis and cuticle (*c.* 30%), with a far lesser role of bundle sheath, bundle sheath extensions, and minor veins (Fig. 2b; Table S11).

Resolving the anatomical and compositional basis for species differences in LMA

The EXACT equations allowed analysis of the anatomical and compositional determinants of species differences in LMA. The important intrinsic drivers of LMA, i.e. those for which an increase in 10% caused > 2% increase in LMA, with all other traits being held constant at their mean values for our species set, were ρ_{cell} and the numbers of spongy and palisade mesophyll cell layers (Fig. 2c; Table S6). When we analysed the shifts in LMA resulting from increasing cell sizes simultaneously throughout the mesophyll and epidermis, given their allometric relationships across species (John *et al.* 2013), cell volume too was an important driver of LMA, with a 10% increase in cell size producing a 2.5% increase in LMA (Fig 2c). By contrast, the other variables, including airspace fraction, cuticle thickness and vein volume per leaf area had relatively negligible intrinsic influences on LMA (Table S6).

Beyond intrinsic sensitivity, we quantified which factors were important realised determinants of LMA variation among the 11 woody species. Any anatomical trait can potentially drive a large shift in LMA (Fig. 2d; Table S7), but across all combinations of species certain traits had primary importance. The traits accounting for > 5% of the across species variation in LMA were ρ_{cell}, mesophyll cell layers and volumes, major vein volume per area and the dry mass density of veins.

Correlational analyses were not reliable for indicating the intrinsic or realised sensitivity of LMA to underlying anatomical or compositional variables (Fig 2e; Table S8). On the one hand, consistent with our intrinsic sensitivity analysis, LMA was correlated across species with ρ_{cell} and numbers of cell layers in the spongy mesophyll. On the other hand, LMA was also significantly correlated across species with several traits that were *not* important intrinsic or realised determinants of LMA, e.g. volume per area of bundle sheath extensions, the number of cell layers in upper epidermis and upper cuticle thickness. Conversely, cell volume was an important intrinsic and realised determinant of LMA yet was not correlated with LMA across our species (Fig. 2c–e). In previous correlational studies (Table 1), LMA was likewise sometimes uncorrelated with traits that are strong intrinsic determinants, e.g. the cell size and numbers of cell layers, and LMA was sometimes correlated across species with traits with very low or negligible intrinsic influence on LMA including cuticle thickness and minor vein length per area (Table 1).

Resolving the anatomical and compositional basis for LMA differences between evergreen and deciduous species

We applied the EXACT equations to clarify the basis for the higher LMA of evergreen than deciduous species (n = 16 and
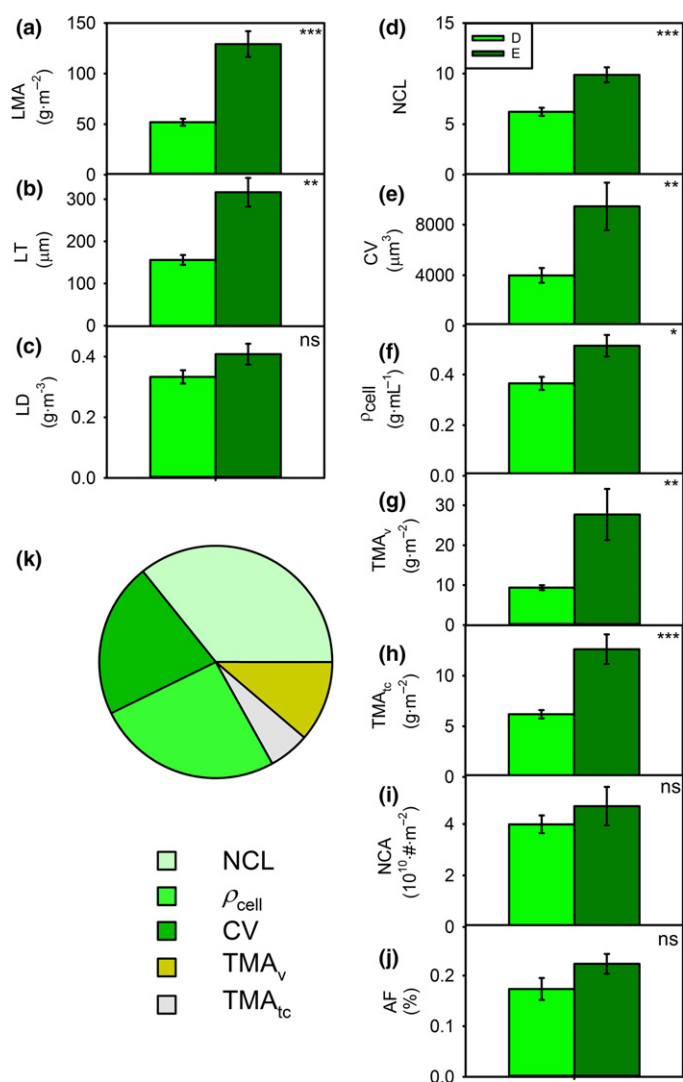
21 respectively; Table S9; Fig. 3a). The evergreen species were greater in ρ_{cell}, numbers of cell layers, cell volume and vein and cuticle mass per area (Fig. 3d–j). According to our realised sensitivity analysis, the variation in LMA was driven in order of decreasing importance by total number of cell layers (36%), ρ_{cell} (26%), cell volume (22%) and the mass of major and minor veins (11%) and cuticle (6%) (Fig. 3k).

Scaling up the influence of anatomical and compositional to the worldwide leaf economics spectrum

Using the EXACT equations we estimated the potential influence of anatomical and compositional traits on other leaf economics spectrum (LES) traits via LMA using available models (Supporting Information Discussion). Variation in anatomical and compositional traits generated LMA values covering 94–100% of the ranges in the global database of photosynthetic and respiration rates and leaf nitrogen concentration per unit leaf mass, and yielded the central trends for the global trait relationships (Fig. S4a–g).

DISCUSSION

The EXACT approach provided unprecedented power to explain LMA. Across the 11 diverse woody angiosperm species, LMA was explained with high accuracy ($R^2 = 0.94$, $P < 0.001$), even with simplifications such as a constant ρ_{cell}. Furthermore, the EXACT approach enabled resolution of leaf design principles, analysis of the determination of species variation in LMA by leaf anatomy and composition, and scaling

up from diversity in leaf anatomy and composition to global leaf economics relationships.

New ability to partition LMA by mass and volume

Applying the EXACT approach provided quantitative insight into leaf design. Across the 11 diverse woody angiosperm species, 25–47% of the leaf volume and mass were accounted for by the photosynthetic mesophyll (spongy and palisade), and 53–75% by supportive structures, including, in order of importance to mass, epidermis, major veins, cuticle, bundle sheath, bundle sheath extensions and minor veins. The resulting volume and mass partitioning show much similarity (as seen by comparing Fig. 2a and b), with mesophyll and major veins being the most influential determinants. However, volume and mass partitioning are not entirely the same even given the assumption of a constant lamina cell dry mass

Figure 2 Establishing drivers of species differences in LMA. Average partitioning of (a) volume and (b) mass of tissues within leaf lamina of diverse woody angiosperm species, highlighting the substantial allocation to space and mass of the photosynthetic mesophyll, and the small contribution of the minor veins ($n = 11$ species). Tissues include palisade and spongy mesophyll (PA and SP respectively), bundle sheath (BS), bundle sheath extension (BSE), upper and lower epidermis (UE and LE respectively), total cuticle (TC), major veins (i.e. first, second and third order; V_{maj}) and minor veins (V_{min}); airspace fraction (AF) also contributes to volume. See Table S4 for values and Table S11 for species mean values. Panels (c) to (e) show the causative influence of traits on LMA and the correlation of LMA with anatomical and compositional traits (trait symbols as in Table 2). (c) intrinsic (mathematical) sensitivity of LMA to each variable; values represent the percent shift in LMA given a 10% shift in each variable, all else held equal; (d) Realised sensitivity of LMA to each variable determined as the median contributions of each parameter to increases in LMA across every pairwise species combination; (e) Pearson correlation coefficients fitted for traits against empirically derived LMA across species; asterisks indicate significance at $p < 0.05$ for both Spearman and Pearson correlations. In (c) and (d) CV for 'all-tissues' represents the sensitivity of LMA to shifting cell volumes across all tissues together; in (e) the all-tissue values represent correlation coefficients of LMA with mean cell size across all tissues. Grey lines show interquartile ranges. Columns in all panels are arranged according to the size of their intrinsic influence on LMA (panel (c)). Bar colour: light green, epidermal anatomical traits; dark green, mesophyll anatomical traits; yellow, vascular anatomical traits; grey, cuticle anatomical traits; white, airspaces; blue, dry mass density; brown, anatomy across lamina tissues. Airspace fraction was the only variable that, when increased, led to a decrease in LMA.

Figure 3 (a–j) Comparison of leaf mass per area and its underlying variables for 21 evergreen and 16 deciduous species (symbols as in Table 2). Significance shown from one-way ANOVAS: *$P < 0.05$, **$P < 0.01$, ***$P < 0.001$; not significant at $P < 0.05$. Number of cell layers (d) and number of cells per area (i) represent the total across tissues for the entire leaf, whereas cell volume (e) is the mean across tissues. (k) Partitioning the influence of anatomical and compositional traits on the variation in leaf mass per area (LMA) between 21 evergreen and 16 deciduous species with the EXACT model. Airspace fraction was not included in panel (k), given it had a negligible negative influence on LMA. We did not have data to quantify the role of vein protrusion, bundle sheath or bundle sheath extensions for this comparison.

density across mesophyll and epidermis. Airspace is the most obvious difference, contributing to volume but not mass, and cuticle, major veins and spongy mesophyll contribute disproportionately to mass relative to their volume.

Higher resolution of the drivers of LMA from underlying anatomical and compositional traits

Our sensitivity analyses showed that the strongest drivers for species differences in LMA were ρ_{cell}, number of cell layers and cell volume (Fig. 2c and d).

In its predictive power, the EXACT approach outperformed models that explained LMA from fewer traits, i.e. the vein origin hypothesis (Blonder *et al.* 2011) and cell wall: protoplast volume hypothesis (Shipley *et al.* 2006). In practice, the explanatory power of these earlier models was based on the information contained in leaf thickness (LT), which is an input of those models. In contrast, the EXACT approach requires explicit inputs of physical dimensions of cells and tissues and mass densities rather than LT. In testing the EXACT approach alongside other models, simplifying assumptions were used (e.g. a constant ρ_{cell} across species), and given additional information future applications could gain even greater accuracy.

Our sensitivity analyses showed that ρ_{cell}, the number of cell layers and cell volume were the most important *intrinsic* drivers of LMA and the major vein volume per area was an additional strong *realised* driver of LMA across our 11 species (Fig. 2c and d). The finding that large cell size drives greater LMA refutes the hypothesis that small cell size should directly drive a higher LMA. That idea was derived from the assumption that most leaf mass is in cell walls, and thus, smaller-celled leaves should have more concentrated mass, but compositional studies show that protoplast components contribute at least equally to leaf mass as cell walls (Villar *et al.* 2006). The finding that LMA is not intrinsically sensitive to the minor vein volume or mass per leaf area refutes the hypothesis that across woody dicotyledons LMA is strongly driven by minor vein traits or by total vein length per area (VLA), which is generally approximated by minor vein length per area. The major veins accounted for a significant minority of LMA, highlighting the importance of considering the hierarchy of vein orders in estimating the contribution of veins to LMA across diverse species. While VLA is not a significant mechanistic driver of LMA across woody dicotyledons, and the two traits are typically independent in correlational analyses (Sack *et al.* 2013, 2014; Li *et al.* 2015), VLA can contribute strongly to area- and mass-based water and carbon flux rates (Sack & Frole 2006; Brodribb *et al.* 2007; Walls 2011; Blonder *et al.* 2011; Sack *et al.* 2013, 2014).

The correlations of LMA with anatomy were only partially consistent with the intrinsic and realised anatomical and compositional determinants, demonstrating the axiom that 'correlation does not imply direct causation', and the importance of an anatomically explicit approach. Indeed, LMA was not correlated across the 11 diverse species with one of its principal intrinsic and realised determinants, cell volume, due to the confounding influence of other factors (Fig. 2c–e). Furthermore, across species, LMA was correlated with several traits that were not intrinsic or realised determinants of LMA, including cuticle and bundle sheath extension volume per area. These trait correlations with LMA likely reflect co-selection for biomechanical support, mechanical protection and leaf longevity (Onoda *et al.* 2011; Méndez-Alonzo *et al.* 2013).

The EXACT approach also clarified how the compositional and anatomical traits that drive LMA relate to leaf thickness (LT) and leaf density (LD). For example the number of cell layers influences LT but not LD, whereas the ρ_{cell} and AF directly influence LD but not LT. All else

being equal a higher cell volume (CV) would increase LT and LMA, though it would potentially reduce LD marginally by diluting the denser tissues such as vein and cuticle (Table S3). These conflicting influences of anatomical traits on LT and LD explain why species sets vary in which is the strongest determinant of LMA: e.g. if species differ strongly in CV with all else similar, then LT will be the strongest driver of high LMA, whereas if species differ strongly in ρ_{cell} or AF with all else similar, then LD will be the major determinant of LMA.

Differences among evergreen and deciduous species

By applying a simplified version of the EXACT approach we revealed that the higher LMA of evergreen species was principally due to higher NCL, ρ_{cell} and CV. These findings should be confirmed within lineages in which evergreen-deciduous shifts occurred.

Scaling up the influence of anatomical and composition to the worldwide leaf economics spectrum

We tested the degree that underlying anatomical and compositional traits can scale up via LMA to play a role in leaf economic spectrum (LES) relationships. Across species, LMA tends to be negatively correlated with nitrogen concentration per mass (N_{mass}), light-saturated photosynthetic rate per mass (A_{mass}) and respiration rate per mass (R_{mass}), and positively related to leaf lifespan (LL) (Small 1972; Reich *et al.* 1997; Wright *et al.* 2004). Applying the EXACT equations to anatomical and compositional traits and applying models for estimating other LES variables from LMA we arrived at values that spanned 94–100% of the range for A_{mass}, N_{mass}, R_{mass} and LL in a global database, and recapitulated the central trend for the global LES relationships (Supporting Information Discussion; Fig. S4a–g). Anatomical and compositional traits may also have direct influence on the other LES traits independently of LMA. Notably, in many species sets, the LES relationships can be weak, as higher A_{mass}, N_{mass} and LL can be achieved at a given LMA for various mechanistic reasons (Fig. S4; Grubb 2016). Use of the EXACT approach to LMA with analogous future extensions of this approach to the anatomical and compositional basis for other LES variables (e.g. Tosens *et al.* 2012; Tomás *et al.* 2013) will elucidate the network of traits that mechanistically determine LES relationships, and the departure from these relationships in given species and clades.

Additional applications of the EXACT approach

The EXACT approach can be extended to a range of potential applications, including:

1 The anatomical and compositional sources of LMA variation across ecological and evolutionary contexts. The EXACT approach can be applied to determine the cell and tissue-level drivers of LMA variation among species within and among communities, within given evolutionary lineages, or possessing contrasting leaf types. These analyses can resolve the sources of plastic variation in LMA among leaves within canopies, or populations of a species across habitats (e.g. sun vs. shade), or for crop varieties developed for greater productivity or stress tolerance. In some comparisons, LMA variation may be strongly driven by features not found important across our sample of species. For example in grasses or conifer needles, the importance of major vein mass would be greater than in dicotyledonous leaves. Furthermore, within sets of leaves that are similar in many traits, e.g. among genotypes of a species, LMA differences might be more strongly determined by traits considered here to be minor, such as cuticle thickness.

2 The estimation of bulk lamina cell dry mass density (ρ_{cell}) as a potential key ecological trait. The application of eqn 8 to estimate ρ_{cell} from LMA and anatomical measurements will enable the testing of the relationship of this trait to cell wall thickness and composition, structural and non-structural carbon, and osmotic concentration, properties with key roles in determining plant ecological processes such as herbivore resistance and drought tolerance (Niinemets 2001; Hanley *et al.* 2007; Hallik *et al.* 2009).

3 The role of additional features in determining LMA. The formulation of the EXACT approach described here focused on features that contribute importantly to LMA to achieve both parsimony and accuracy (Gauch 2003). When LMA depends strongly on additional features, these can be added to the EXACT approach. For example in some populations of Californian *Encelia farinosa* or Hawaiian tree *Metrosideros polymorpha*, trichome mass per area accounts for up to 60% of LMA (Ehleringer & Cook 1984; Hoof *et al.* 2008; Tsujii *et al.* 2016). The approach could also be expanded to include the rachis of compound leaves (cf. Niinemets *et al.* 2006). Furthermore, given traits can be further partitioned. When data are available, it will also be essential to include the mass densities of individual lamina tissues rather than bulk ρ_{cell}, which would further improve the predictive power of the approach. In addition, one might consider the cell wall separately from the protoplast, and analyse their mass densities in terms of their chemical constituents, e.g. carbohydrates, proteins, lignin, minerals, etc. (Villar *et al.* 2006).

4 The anatomical and compositional basis for LMA relationships with other traits and climate. LMA relationships are among the best-known macroecological trends. For example across diverse species, LMA is often positively related to leaf size, a trend known as the 'diminishing returns' of leaf area with increasing leaf mass (Milla & Reich 2007; Niklas *et al.* 2007, 2009). In addition, higher LMA is related to greater aridity in some species sets (Niinemets 2001; Wright *et al.* 2005), but not others (Bartlett *et al.* 2012; Maréchaux *et al.* 2015). Future studies can analyse if these trends in LMA are associated with denser cells, larger cells, a greater number of cell layers or greater major vein allocation.

5 Detailed causal analyses or evolutionary hypotheses for the determination of LMA. Previous studies have postulated causal networks for LMA, including not only underlying drivers such as anatomy and composition, but also constraints on gross leaf structure, which could affect which anatomical variables would shift given selection on LMA (Shipley *et al.* 2006; Blonder *et al.* 2015). The EXACT approach can be utilised to

refine and test the effects of such constraints. For instance one might test the effect of keeping leaf thickness constant to reflect selection to maintain effective light absorption while varying cell size; given that constraint, the number of cell layers will shift to counteract cell size, and there would arise little overall relationship between cell size and LMA across species (Pyankov *et al.* 1999). With the EXACT model, simulations of such hypotheses can be applied to generate and test explicit predictions.

Extending this explicit quantitative framework to a wide array of species, considering additional anatomical, compositional, biochemical and physiological traits, and relating these underlying variables to a wider set of upper level traits will contribute to next-generation understanding for scaling from leaf diversity to function and to ecological diversification worldwide.

ACKNOWLEDGEMENTS

AUTHOR CONTRIBUTIONS

GJ and LS designed the study. GJ, CS, RV and HP collected anatomical and compositional data. GJ, LS and TB conducted analyses. GJ and LS wrote the paper with contributions from all authors.

REFERENCES

Adler, P.B., Salguero-Gomez, R., Compagnoni, A., Hsu, J.S., Ray-Mukherjee, J., Mbeau-Ache, C. *et al.* (2014). Functional traits explain variation in plant life history strategies. *Proc. Natl Acad. Sci. USA*, 111, 740–745.

Aranda, I., Pardo, F., Gil, L. & Pardos, J.A. (2004). Anatomical basis of the change in leaf mass per area and nitrogen investment with relative irradiance within the canopy of eight temperate tree species. *Acta Oecologica*, 25, 187–195.

Bartlett, M.K., Scoffoni, C. & Sack, L. (2012). The determinants of leaf turgor loss point and prediction of drought tolerance of species and biomes: a global meta-analysis. *Ecol. Lett.*, 15, 393–405.

Blonder, B., Baldwin, B.G., Enquist, B.J. & Robichaux, R.H. (2016). Variation and macroevolution in leaf functional traits in the Hawaiian silversword alliance (Asteraceae). *Journal of Ecology*, 104, 219–228.

Blonder, B., Violle, C., Bentley, L.P. & Enquist, B.J. (2011). Venation networks and the origin of the leaf economics spectrum. *Ecol. Lett.*, 14, 91–100.

Blonder, B., Vasseur, F., Violle, C., Shipley, B., Enquist, B.J. & Vile, D. (2015). Testing models for the leaf economics spectrum with leaf and whole-plant traits in *Arabidopsis thaliana*. *Aob Plants*, 7.

Brodribb, T.J., Jordan, G.J. & Carpenter, R.J. (2013). Unified changes in cell size permit coordinated leaf evolution. *New Phytologist*, 199, 559–570.

Brodribb, T.J., Feild, T.S. & Jordan, G.J. (2007). Leaf maximum photosynthetic rate and venation are linked by hydraulics. *Plant Physiol.*, 144, 1890–1898.

Buckley, T.N. & Diaz-Espejo, A. (2015). Partitioning changes in photosynthetic rate into contributions from different variables. *Plant, Cell Environ.*, 38, 1200–1211.

Castro-Diez, P., Puyravaud, J.P. & Cornelissen, J.H.C. (2000). Leaf structure and anatomy as related to leaf mass per area variation in seedlings of a wide range of woody plant species and types. *Oecologia*, 124, 476–486.

Chatelet, D.S., Clement, W.L., Sack, L., Donoghue, M.J. & Edwards, E.J. (2013). The evolution of photosynthetic anatomy in *Viburnum* (Adoxaceae). *Int. J. Plant Sci.*, 174, 1277–1291.

Cornelissen, J.H.C. & Thompson, K. (1997). Functional leaf attributes predict litter decomposition rate in herbaceous plants. *New Phytol.*, 135, 109–114.

Cornwell, W.K., Cornelissen, J.H.C., Amatangelo, K., Dorrepaal, E., Eviner, V.T., Godoy, O. *et al.* (2008). Plant species traits are the predominant control on litter decomposition rates within biomes worldwide. *Ecol. Lett.*, 11, 1065–1071.

de la Riva, E.G., Olmo, M., Poorter, H., Ubera, J.L. & Villar, R. (2016). Leaf mass per area (LMA) and its relationship with leaf structure and anatomy in 34 Mediterranean woody species along a water availability gradient. *PLoS One*, 11.

Diaz, S., Kattge, J., Cornelissen, J.H.C., Wright, I.J., Lavorel, S., Dray, S. *et al.* (2016). The global spectrum of plant form and function. *Nature*, 529, 167–U73.

Dunbar-Co, S., Sporck, M.J. & Sack, L. (2009). Leaf trait diversification and design in seven rare taxa of the Hawaiian Plantago radiation. *International Journal of Plant Sciences*, 170, 61–75.

Ehleringer, J.R. & Cook, C.S. (1984). Photosynthesis in *Encelie farinosa* Gray in response to decreasing leaf water potential. *Plant Physiol.*, 75, 688–693.

Funk, J.L. & Cornwell, W.K. (2013). Leaf traits within communities: context may affect the mapping of traits to function. *Ecology*, 94, 1893–1897.

Garnier, E. & Laurent, G. (1994). Leaf anatomy, specific mass and water content in congeneric annual and perennial grass species. *New Phytologist*, 128, 725–736.

Gauch, H.G. (2003). *Scientific Method in Practice*. Cambridge University Press, New York.

Grubb, P.J. (2016). Trade-offs in interspecific comparisons in plant ecology and how plants overcome proposed constraints. *Plant Ecol. Divers*, 9, 3–33.

Gurevitch, J., Scheiner, S.M. & Fox, G.A. (2002). *The Ecology of Plants*, 2nd edn. Sinauer Associates Inc, Publishers, Sunderland, MA.

Hallik, L., Niinemets, U. & Wright, I.J. (2009). Are species shade and drought tolerance reflected in leaf-level structural and functional differentiation in Northern Hemisphere temperate woody flora? *New Phytol.*, 184, 257–274.

Hanley, M.E., Lamont, B.B., Fairbanks, M.M. & Rafferty, C.M. (2007). Plant structural traits and their role in anti-herbivore defence. *Perspect. Plant Ecol. Evol. Syst.*, 8, 157–178.

Herben, T., Suda, J., Klimesova, J., Mihulka, S., Riha, P. & Simova, I. (2012). Ecological effects of cell-level processes: genome size, functional traits and regional abundance of herbaceous plant species. *Ann. Bot.*, 110, 1357–1367.

Hoof, J., Sack, L., Webb, D.T. & Nilsen, E.T. (2008). Contrasting structure and function of pubescent and glabrous varieties of Hawaiian *Metrosideros polymorpha* (Myrtaceae) at high elevation. *Biotropica*, 40, 113–118.

John, G.P., Scoffoni, C. & Sack, L. (2013). Allometry of cells and tissues within leaves. *Am. J. Bot.*, 100, 1936–1948.

Kawai, K. & Okada, N. (2016). How are leaf mechanical properties and water-use traits coordinated by vein traits? *A Case Study in Fagaceae*. *Functional Ecology*, 30, 527–536.

Kunstler, G., Falster, D., Coomes, D.A., Hui, F., Kooyman, R.M., Laughlin, D.C. *et al.* (2016). Plant functional traits have globally consistent effects on competition. *Nature*, 529, 204–U174.

Li, L., McCormack, M.L., Ma, C.G., Kong, D.L., Zhang, Q., Chen, X.Y. et al. (2015). Leaf economics and hydraulic traits are decoupled in five species-rich tropical-subtropical forests. *Ecol. Lett.*, 18, 899–906.

Maréchaux, I., Bartlett, M.K., Sack, L., Baraloto, C., Engel, J., Joetzjer, E. et al. (2015). Drought tolerance as predicted by leaf water potential at turgor loss point varies strongly across species within an Amazonian forest. *Funct. Ecol.*, 29, 1268–1277.

Mason, C.M. & Donovan, L.A. (2015). Evolution of the leaf economics spectrum in herbs: evidence from environmental divergences in leaf physiology across *Helianthus* (Asteraceae). *Evolution*, 69, 2705–2720.

Méndez-Alonzo, R., Ewers, F.W. & Sack, L. (2013). Ecological variation in leaf biomechanics and its scaling with tissue structure across three mediterranean-climate plant communities. *Funct. Ecol.*, 27, 544–554.

Milla, R. & Reich, P.B. (2007). The scaling of leaf area and mass: the cost of light interception increases with leaf size. *Proc. R. Soc. B Biol. Sci.*, 274, 2109–2114.

Niinemets, U. (1999). Components of leaf dry mass per area - thickness and density - alter leaf photosynthetic capacity in reverse directions in woody plants. *New Phytol.*, 144, 35–47.

Niinemets, U. (2001). Global-scale climatic controls of leaf dry mass per area, density, and thickness in trees and shrubs. *Ecology*, 82, 453–469.

Niinemets, U., Portsmuth, A. & Tobias, M. (2006). Leaf size modifies support biomass distribution among stems, petioles and mid-ribs in temperate plants. *New Phytol.*, 171, 91–104.

Niklas, K.J., Cobb, E.D., Niinemets, U., Reich, P.B., Sellin, A., Shipley, B. et al. (2007). "Diminishing returns" in the scaling of functional leaf traits across and within species groups. *Proc. Natl Acad. Sci. USA*, 104, 8891–8896.

Niklas, K.J., Cobb, E.D. & Spatz, H.-C. (2009). Predicting the allometry of leaf surface area and dry mass. *Am. J. Bot.*, 96, 531–536.

Nobel, P.S. (2009). *Physicochemical and Environmental Plant Physiology*, 5th edn. Academic Press, San Diego.

Onoda, Y., Westoby, M., Adler, P.B., Choong, A.M.F., Clissold, F.J., Cornelissen, J.H.C. et al. (2011). Global patterns of leaf mechanical properties. *Ecol. Lett.*, 14, 301–312.

Perez-Harguindeguy, N., Diaz, S., Garnier, E., Lavorel, S., Poorter, H., Jaureguiberry, P. et al. (2013). New handbook for standardised measurement of plant functional traits worldwide. *Aust. J. Bot.*, 61, 167–234.

Poorter, H. and Van der Werf, A. (1998). Is inherent variation in RGR determined by LAR at low irradiance and by NAR at high irradiance? A review of herbaceous species. In: *Inherent Variation in Plant Growth. Physiological Mechanisms and Ecological Consequences* (eds H., Lambers, H., Poorter and M.M.I., van Vuuren.). Leiden, the Netherlands: Backhuys Publishers, pp. 309–336.

Poorter, H., Niinemets, U., Poorter, L., Wright, I.J. & Villar, R. (2009). Causes and consequences of variation in leaf mass per area (LMA): a meta-analysis. *New Phytol.*, 182, 565–588.

Pyankov, V.I., Kondratchuk, A.V. & Shipley, B. (1999). Leaf structure and specific leaf mass: the alpine desert plants of the Eastern Pamirs, Tadjikistan. *New Phytol.*, 143, 131–142.

Richardson, S.J., Allen, R.B., Buxton, R.P., Easdale, T.A., Hurst, J.M., Morse, C.W., Smissen, R.D. & Peltzer, D.A. (2013). Intraspecific relationships among wood density, leaf structural traits and environment in four co-occurring species of Nothofagus in New Zealand. *PLoS One*, 8.

Reich, P.B. (2001). Body size, geometry, longevity and metabolism: do plant leaves behave like a animal bodies? *Trends Ecol. Evol.*, 16, 675–680.

Reich, P.B. (2014). The world-wide 'fast-slow' plant economics spectrum: a traits manifesto. *J. Ecol.*, 102, 275–301.

Reich, P.B., Walters, M.B. & Ellsworth, D.S. (1997). From tropics to tundra: global convergence in plant functioning. *Proc. Natl Acad. Sci. USA*, 94, 13730–13734.

Richardson, S.J., Allen, R.B., Buxton, R.P., Easdale, T.A., Hurst, J.M., Morse, C.W. et al. (2013). Intraspecific relationships among wood density, leaf structural traits and environment in four co-occurring species of Nothofagus in New Zealand. *PLoS ONE*, 8.

Ronzhina, D.A. & Ivanov, L.A. (2014). Construction costs and mesostructure of leaves in hydrophytes. *Russian Journal of Plant Physiology*, 61, 776–783.

Roderick, M.L., Berry, S.L., Noble, I.R. & Farquhar, G.D. (1999a). A theoretical approach to linking the composition and morphology with the function of leaves. *Funct. Ecol.*, 13, 683–695.

Roderick, M.L., Berry, S.L., Saunders, A.R. & Noble, I.R. (1999b). On the relationship between the composition, morphology and function of leaves. *Funct. Ecol.*, 13, 696–710.

Sack, L. & Frole, K. (2006). Leaf structural diversity is related to hydraulic capacity in tropical rain forest trees. *Ecology*, 87, 483–491.

Sack, L., Cowan, P.D., Jaikumar, N. & Holbrook, N.M. (2003). The 'hydrology' of leaves: co-ordination of structure and function in temperate woody species. *Plant, Cell Environ.*, 26, 1343–1356.

Sack, L., Scoffoni, C., McKown, A.D., Frole, K., Rawls, M., Havran, J.C. et al. (2012). Developmentally based scaling of leaf venation architecture explains global ecological patterns. *Nat. Commun.*, 3, 1–10.

Sack, L., Scoffoni, C., John, G.P., Poorter, H., Mason, C.M., Mendez-Alonzo, R. et al. (2013). How do leaf veins influence the worldwide leaf economic spectrum? Review and synthesis. *J. Exp. Bot.*, 64, 4053–4080.

Sack, L., Scoffoni, C., John, G.P., Poorter, H., Mason, C.M., Mendez-Alonzo, R. & Donovan, L.A. (2013). How do leaf veins influence the worldwide leaf economic spectrum? Review and synthesis. *Journal of Experimental Botany*, 64, 4053–4080.

Sack, L., Scoffoni, C., John, G.P., Poorter, H., Mason, C.M., Mendez-Alonzo, R. et al. (2014). Leaf mass per area is independent of vein length per area: avoiding pitfalls when modelling phenotypic integration. *J. Exp. Bot.*, 65, 5115–5123.

Scoffoni, C., Kunkle, J., Pasquet-Kok, J., Vuong, C., Patel, A.J., Montgomery, R.A., Givnish, T.J. & Sack, L. (2015). Light-induced plasticity in leaf hydraulics, venation, anatomy, and gas exchange in ecologically diverse Hawaiian lobeliads. *New Phytologist*, 207, 43–58.

Scoffoni, C., Rawls, M., McKown, A., Cochard, H. & Sack, L. (2011). Decline of leaf hydraulic conductance with dehydration: relationship to leaf size and venation architecture. *Plant Physiol.*, 156, 832–843.

Shipley, B. (1995). Structured interspecific determinants of specific leaf area in 34 species of herbaceous angiosperms. *Funct. Ecol.*, 9, 312–319.

Shipley, B., Lechowiecz, M.J., Wright, I. & Reich, P.B. (2006). Fundamental trade-offs generating the worldwide leaf economics spectrum. *Ecology*, 87, 535–541.

Small, E. (1972). Photosynthetic rates in relation to nitrogen recycling as an adaptation to nutrient deficiency in peat bog plants. *Can. J. Bot.*, 50, 2227–2233.

Tomás, M., Flexas, J., Copolovici, L., Galmés, J., Hallik, L., Medrano, H. et al. (2013). Importance of leaf anatomy in determining mesophyll diffusion conductance to CO_2 across species: quantitative limitations and scaling up by models. *J. Exp. Bot.*, 64, 2269–2281.

Tosens, T., Niinemets, U., Westoby, M. & Wright, I.J. (2012). Anatomical basis of variation in mesophyll resistance in eastern Australian sclerophylls: news of a long and winding path. *J. Exp. Bot.*, 63, 5105–5119.

Tsujii, Y., Onoda, Y., Izuno, A., Isagi, Y. & Kitayama, K. (2016). A quantitative analysis of phenotypic variations of *Metrosideros polymorpha* within and across populations along environmental gradients on Mauna Loa, Hawaii. *Oecologia*, 180, 1049–1059.

Uhl, D. & Mosbrugger, V. (1999). Leaf venation density as a climate and environmental proxy: a critical review and new data. *Palaeogeogr. Palaeoclimatol. Palaeoecol.*, 149, 15–26.

Van Arendonk, J.J.C.M., Niemann, G.J., Boon, J.J. & Lambers, H. (1997). Effects of nitrogen supply on the anatomy and chemical composition of leaves of four grass species belonging to the genus *Poa*, as determined by image-processing analysis and pyrolysis mass spectrometry. *Plant Cell and Environment*, 20, 881–897.

Van Arendonk, J.J.C.M. & Poorter, H. (1994). The chemical composition and anatomical structure of leaves of grass species differing in relative growth rate. *Plant Cell and Environment*, 17, 963–970.

Villar, R. & Merino, J. (2001). Comparison of leaf construction costs in woody species with differing leaf life-spans in contrasting ecosystems. *New Phytol.*, 151, 213–226.

Villar, R., Robleto, J.R., De Jong, Y. & Poorter, H. (2006). Differences in construction costs and chemical composition between deciduous and evergreen woody species are small as compared to differences among families. *Plant, Cell Environ.*, 29, 1629–1643.

Villar, R., Ruiz-Robleto, J., Ubera, J.L. & Poorter, H. (2013). Exploring variation in leaf mass per area (LMA) from leaf to cell: an anatomical analysis of 26 woody species. *Am. J. Bot.*, 100, 1969–1980.

Wagenmakers, E.J. (2003). Model selection and multimodel inference: a practical information-theoretic approach. *J. Math. Psychol.*, 47, 580–586.

Walls, R.L. (2011). Angiosperm leaf vein patterns are linked to leaf functions in a global-scale data set. *Am. J. Bot.*, 98, 244–253.

Wang, R., Yu, G., He, N., Wang, Q., Zhao, N., Xu, Z. *et al.* (2015). Latitudinal variation of leaf stomatal traits from species to community level in forests: linkage with ecosystem productivity. *Sci. Rep.*, 5, 1–11.

Warton, D.I., Wright, I.J., Falster, D.S. & Westoby, M. (2006). Bivariate line-fitting methods for allometry. *Biol. Rev.*, 81, 259–291.

Westoby, M., Falster, D.S., Moles, A.T., Vesk, P.A. & Wright, I.J. (2002). Plant ecological strategies: Some leading dimensions of variation between species. *Annu. Rev. Ecol. Syst.*, 33, 125–159.

Witkowski, E.T.F. & Lamont, B.B. (1991). Leaf specific mass confounds leaf density and thickness. *Oecologia*, 88, 486–493.

Wright, I.J., Reich, P.B., Westoby, M., Ackerly, D.D., Baruch, Z., Bongers, F. *et al.* (2004). The worldwide leaf economics spectrum. *Nature*, 428, 821–827.

Wright, I.J., Reich, P.B., Cornelissen, J.H.C., Falster, D.S., Groom, P.K., Hikosaka, K. *et al.* (2005). Modulation of leaf economic traits and trait relationships by climate. *Glob. Ecol. Biogeogr.*, 14, 411–421.

Xiong, D.L., Yu, T.T., Zhang, T., Li, Y., Peng, S.B. & Huang, J.L. (2015). Leaf hydraulic conductance is coordinated with leaf morpho-anatomical traits and nitrogen status in the genus *Oryza*. *Journal of Experimental Botany*, 66, 741–748.

SUPPORTING INFORMATION

Additional Supporting Information may be found online in the supporting information tab for this article.